

SPECTRAL THEORY OF EFFECTIVE TRANSPORT FOR DISCRETE UNIAXIAL POLYCRYSTALLINE MATERIALS

N. BENJAMIN MURPHY, DANIEL HALLMAN, ELENA CHERKAEV, AND KENNETH M. GOLDEN

Department of Mathematics, University of Utah, 155 S 1400 E, Salt Lake City, UT 84112-0090

ABSTRACT. We previously demonstrated that the bulk transport coefficients of uniaxial polycrystalline materials, including electrical and thermal conductivity, diffusivity, complex permittivity, and magnetic permeability, have Stieltjes integral representations involving spectral measures of self-adjoint random operators. The integral representations follow from resolvent representations of physical fields involving these self-adjoint operators, such as the electric field \mathbf{E} and current density \mathbf{J} associated with conductive media with local conductivity $\boldsymbol{\sigma}$ and resistivity $\boldsymbol{\rho}$ matrices. In this article, we provide a discrete matrix analysis of this mathematical framework which parallels the continuum theory. We show that discretizations of the operators yield real-symmetric random matrices which are composed of projection matrices. We derive discrete resolvent representations for \mathbf{E} and \mathbf{J} involving the matrices which lead to eigenvector expansions of \mathbf{E} and \mathbf{J} . We derive discrete Stieltjes integral representations for the components of the effective conductivity and resistivity matrices, $\boldsymbol{\sigma}^*$ and $\boldsymbol{\rho}^*$, involving spectral measures for the real-symmetric random matrices, which are given explicitly in terms of their real eigenvalues and orthonormal eigenvectors. We provide a projection method that uses properties of the projection matrices to show that the spectral measure can be computed by much smaller matrices, which leads to a more efficient and stable numerical algorithm for the computation of bulk transport coefficients and physical fields. We demonstrate this algorithm by numerically computing the spectral measure and current density for model 2D and 3D isotropic polycrystalline media with checkerboard microgeometry.

1. INTRODUCTION

In [26] we formulated a mathematical framework to provide Stieltjes integral representations for the bulk transport coefficients for uniaxial polycrystalline materials [1, 15, 22], including electrical and thermal conductivity, diffusivity, complex permittivity, and magnetic permeability, involving spectral measures of self-adjoint random operators. All of these transport phenomena are described locally by the same elliptic partial differential equation (PDE) [22]. For example, static electrical conduction [18] is described by $\nabla \cdot (\boldsymbol{\sigma} \nabla \phi) = 0$ with electrical potential ϕ , electric field $\mathbf{E} = -\nabla \phi$, and local conductivity matrix $\boldsymbol{\sigma}$ given by [22] $\boldsymbol{\sigma} = R^T \text{diag}(\sigma_1, \sigma_2, \dots, \sigma_2) R$ where σ_1 and σ_2 are real-valued, i.e., $\boldsymbol{\sigma} = R^T \text{diag}(\sigma_1, \sigma_2, \sigma_2) R$ for 3D and $\boldsymbol{\sigma} = R^T \text{diag}(\sigma_1, \sigma_2) R$ for 2D. This is the general setting for 2D but introduces a uniaxial asymmetry for $d \geq 3$, i.e., the local conductivity along one of the crystal axes has the value σ_1 , while the conductivity along all the other crystal axes has the value σ_2 . Here, R is a rotation matrix that determines the arrangement and orientations of the crystallites comprising the polycrystalline material.

Consequently, the current and electric fields $\mathbf{J} = \boldsymbol{\sigma} \mathbf{E}$ and \mathbf{E} satisfy the electrostatic version of Maxwell's equations $\nabla \cdot \mathbf{J} = \rho$ and $\nabla \times \mathbf{E} = 0$. In the long electromagnetic wavelength limit, the electric and displacement fields satisfy the quasistatic limit of Maxwell's equations [22] $\nabla \cdot \mathbf{D} = \rho_b$ and $\nabla \times \mathbf{E} = 0$, where ρ_b is the bound charge density [18], the displacement field is given by $\mathbf{D} = \boldsymbol{\epsilon} \mathbf{E}$, $\boldsymbol{\epsilon} = R^T \text{diag}(\epsilon_1, \epsilon_2, \dots, \epsilon_2) R$, and the crystal permittivities $\epsilon_1(f)$ and $\epsilon_2(f)$ take *complex values* which depend on the electromagnetic wave frequency f . In the remainder of this manuscript we formulate the problem of effective transport in terms of electrical conductivity, keeping in mind the broad applicability of the method.

Polycrystalline materials are solids that are composed of many crystallites of varying size, shape, and orientation. The crystallites are microscopic crystals which are held together by boundaries which can be highly defective. Due to the highly irregular shapes of the crystallites and their defective boundaries, on a microscopic level, the electromagnetic transport properties of the medium can be quite erratic. As a consequence, the derivatives in the transport equations may not hold in a classical sense and a weak

formulation of the transport equation is necessary to provide a rigorous mathematical description of effective transport for such materials [27, 14].

In [26] we utilized the mathematical framework developed in [27, 14] to show that the spectral measures underlying the Stieltjes integral representations for the bulk transport coefficients are associated with self-adjoint compositions of random and non-random projection operators. The random projection operators follow from writing $\boldsymbol{\sigma} = R^T \text{diag}(\sigma_1, \sigma_2, \dots, \sigma_2) R$ as $\boldsymbol{\sigma} = \sigma_1 X_1 + \sigma_2 X_2$, where X_1 and X_2 are mutually orthogonal projection matrices that contain geometric information about the polycrystalline material via the rotation matrix R . A non-random projection operator arising in Stieltjes integrals for the components σ_{jk}^* , $i, j = 1, \dots, d$, of the effective electrical conductivity matrix $\boldsymbol{\sigma}^*$ is given by $\Gamma = \nabla(\nabla^* \nabla)^{-1} \nabla^*$, which is a projection onto the range of a generalized gradient operator ∇ , where ∇^* is the adjoint of ∇ and d is the system dimension. The Stieltjes integrals involve spectral measures for the self-adjoint random operators $X_i \Gamma X_i$, $i = 1, 2$. The Stieltjes integrals for the components ρ_{jk}^* , $i, j = 1, \dots, d$, of the effective electrical resistivity matrix $\boldsymbol{\rho}^*$ involve spectral measures for the self-adjoint random operators $X_i \Upsilon X_i$, $i = 1, 2$, where $\Upsilon = \nabla \times (\nabla \times \nabla \times)^{-1} \nabla \times$ is a projection onto the range of a generalized curl operator $\nabla \times$.

Here develop a discrete mathematical framework that closely resembles the mathematical framework for the continuum setting [26], which provides a rigorous way to numerically compute spectral measures, effective parameters, and the physical fields \boldsymbol{E} and \boldsymbol{J} for uniaxial polycrystalline materials. In particular, discretization of a continuous medium leads to a matrix analysis description of effective transport in composites which closely parallels the associated partial differential equation description for the continuum setting. Remarkably, the discrete formulation follows directly from just the fundamental theorem of linear algebra and known [17] orthogonality properties of the domains, ranges, and kernels of discrete, finite difference representations of the curl, gradient, and divergence operators.

In this discrete setting, the random operators $X_i \Gamma X_i$ and $X_i \Upsilon X_i$, $i = 1, 2$, underlying the integral representations for the effective parameters are represented by real-symmetric random matrices. The physical fields \boldsymbol{E} and \boldsymbol{J} and the spectral measures are determined explicitly by their real eigenvalues and orthonormal eigenvectors. We provide a numerically efficient projection method to facilitate such numerical computations, and use the method to compute the physical fields \boldsymbol{E} and \boldsymbol{J} , spectral measures, and effective parameters for a model of isotropic polycrystalline media with checkerboard microgeometry. In 2D, computed spectral measures are in excellent agreement with known theoretical results, and the computed values of the effective parameters fall within the rigorous bounds, as shown in [26].

2. STIELTJES INTEGRALS FOR BULK TRANSPORT COEFFICIENTS FOR CONTINUOUS MEDIA

In this section, we briefly describe the *analytic continuation method* for studying the effective transport properties of composite materials [3, 21, 14, 12]. In particular, we review our application of the method to the setting of uniaxial polycrystalline materials given in [26]. This method has been used to obtain rigorous bounds on bulk transport coefficients of polycrystalline media from partial knowledge of the microstructure, such as the average orientation angle θ of each crystallite [15, 26]. Examples of transport coefficients to which this approach applies include the complex permittivity, electrical and thermal conductivity, diffusivity, and magnetic permeability. To set ideas we focus on electrical conductivity, keeping the broad applicability of the method in mind. Consider a random medium with local conductivity matrix $\boldsymbol{\sigma}(x, \omega)$, a spatially stationary random field in $x \in \mathbb{R}^d$ and $\omega \in \Omega$, where Ω is the set of realizations of the medium.

The local conductivity matrix $\boldsymbol{\sigma}$ for uniaxial polycrystalline materials is given by [1, 15, 22, 26] $\boldsymbol{\sigma} = R^T \text{diag}(\sigma_1, \sigma_2, \dots, \sigma_2) R$, i.e., $\boldsymbol{\sigma} = R^T \text{diag}(\sigma_1, \sigma_2, \sigma_2) R$ for 3D and $\boldsymbol{\sigma} = R^T \text{diag}(\sigma_1, \sigma_2) R$ for 2D, where $R(\boldsymbol{x}, \omega)$ is a random rotation matrix determining the orientation of the crystallite with \boldsymbol{x} in the interior for $\omega \in \Omega$ — this is the general setting for 2D but introduces a uniaxial asymmetry for $d \geq 3$. The orientation of each crystallite comprising the polycrystalline composite material is determined by a single angle $\theta(\boldsymbol{x}, \omega)$ and single rotation matrix for 2D, and d angles $\theta_i(\boldsymbol{x}, \omega)$, $i = 1, \dots, d$ for dimension $d \geq 3$, where R is a composition of simple rotation matrices [26]. Using the projection matrix $C = \text{diag}(\mathbf{e}_1)$, where \mathbf{e}_k is the k th standard basis vector, the local conductivity tensor can be written as

$$(2.1) \quad \boldsymbol{\sigma}(x, \omega) = \sigma_1 X_1(x, \omega) + \sigma_2 X_2(x, \omega).$$

where $X_1 = R^T C R$, $X_2 = R^T (I - C) R$ and I is the identity matrix. The random electric and current fields $\mathbf{E}(x, \omega)$ and $\mathbf{J}(x, \omega)$ satisfy [18]

$$(2.2) \quad \nabla \times \mathbf{E} = 0, \quad \nabla \cdot \mathbf{J} = 0, \quad \mathbf{J} = \sigma \mathbf{E}.$$

We define [26] the effective conductivity matrix σ^* by [27] $\langle \mathbf{J} \rangle = \sigma^* \langle \mathbf{E} \rangle$, where $\langle \cdot \rangle$ is ensemble averaging over Ω or spatial average over all of \mathbb{R}^d [14]. We define our coordinate system so that $\langle \mathbf{E} \rangle = \mathbf{E}_0 = E_0 \mathbf{e}_k$. A variational calculation [14, 26] establishes the energy constraint

$$(2.3) \quad \langle \mathbf{J} \cdot \mathbf{E}_f \rangle = 0$$

(Helmholtz's theorem) involving the fluctuating field $\mathbf{E}_f = \mathbf{E} - \mathbf{E}_0$. It then follows from $\langle \mathbf{J} \cdot \mathbf{E} \rangle = \langle \mathbf{J} \rangle \cdot \mathbf{E}_0$ that σ^* is also given in terms of the energy functional

$$(2.4) \quad \langle \mathbf{J} \cdot \mathbf{E} \rangle = \sigma^* \mathbf{E}_0 \cdot \mathbf{E}_0, \quad \mathbf{E}_0 = E_0 \mathbf{e}_k.$$

Consequently, the method defines a homogeneous medium with constant conductivity matrix σ^* subject to a uniform applied electric field $\mathbf{E}_0 = E_0 \mathbf{e}_k$ with constant electric field strength E_0 that behaves both macroscopically and energetically *exactly the same* as the inhomogeneous polycrystalline material in the infinite volume limit [27].

The key step of the method is to obtain the following Stieltjes integral representation for σ^* [2, 21, 14, 22],

$$(2.5) \quad F_{jk}(s) = 1 - \frac{\sigma_{jk}^*}{\sigma_2} = \int_0^1 \frac{d\mu_{jk}(\lambda)}{s - \lambda}, \quad s = \frac{1}{1 - \sigma_1/\sigma_2},$$

where the μ_{jk} , $j, k = 1, \dots, d$ are Stieltjes measure on $[0, 1]$, the μ_{kk} are *positive* measures and the μ_{jk} for $j \neq k$ are *signed* measures. In the variable $h = \sigma_1/\sigma_2$, $F(s) = \langle X_1 \mathbf{E} \cdot X_1 \mathbf{e}_k \rangle / (s E_0)$ is a *Stieltjes function* [11, 25], playing the role of effective electric susceptibility, $\chi^*(s) = \sigma^*/\sigma_2 - 1 = -F(s)$. Equation (2.5) arises from a resolvent formula for the components of the electric field,

$$(2.6) \quad X_1 \mathbf{E} = s(sI - X_1 \Gamma X_1)^{-1} X_1 \mathbf{E}_0,$$

yielding $F_{jk}(s) = \langle [(sI - X_1 \Gamma X_1)^{-1} X_1 \mathbf{e}_j] \cdot X_1 \mathbf{e}_k \rangle$, where $\Gamma = -\nabla(-\Delta)^{-1}\nabla$ is a projection onto the range of the gradient operator ∇ , where $\Delta = \nabla \cdot \nabla = \nabla^2$ is the Laplacian operator. Formula (2.5) is the spectral representation of the resolvent and μ is the spectral measure of the self-adjoint operator $X_1 \Gamma X_1$ on $L^2(\Omega, P)$. (Stieltjes integral representations for the σ_{jk}^* can also be formulated in terms of the self-adjoint operator $X_2 \Gamma X_2$ and the contrast variable $t = 1/(1 - \sigma_2/\sigma_1) = 1 - s$ [26].)

A key feature of equation (2.5) is that the component parameters, σ_1 and σ_2 , in s are separated from the geometrical information in the spectral measure μ_{jk} . Information about the geometry enters through the moments

$$(2.7) \quad \mu_{jk}^n = \int_0^1 \lambda^n d\mu_{jk}(\lambda) = \langle [X_1 \Gamma X_1]^n X_1 \mathbf{e}_j \cdot X_1 \mathbf{e}_k \rangle.$$

The measure mass is given by $\mu_{jk}^0 = \langle X_1 \mathbf{e}_j \cdot \mathbf{e}_k \rangle$, which can be thought of as the ‘‘mean orientation’’, or as a percentage of crystallites oriented in the k^{th} direction. In general, higher order moments μ_{jk}^n depend on the $(n + 1)$ -point correlation function of the medium [14].

The local resistivity matrix is the matrix inverse of the conductivity matrix, $\rho = \sigma^{-1}$. Stieltjes integral representations for the components ρ_{jk}^* of the effective resistivity matrix ρ^* can be given in terms of the self-adjoint operators $X_1 \Upsilon X_1$ and $X_2 \Upsilon X_2$, where $\Upsilon = \nabla \times (\nabla \times \nabla \times)^{-1} \nabla \times$ is a projection onto the range of the curl operator $\nabla \times$ [26]. Here, the effective resistivity matrix is defined by $\langle \mathbf{E} \rangle = \rho^* \langle \mathbf{J} \rangle$ and we define our coordinate system so that $\langle \mathbf{J} \rangle = \mathbf{J}_0 = J_0 \mathbf{e}_k$. The energy constraint is given by

$$(2.8) \quad \langle \mathbf{J}_f \cdot \mathbf{E} \rangle = 0$$

which leads to the energy functional representation for ρ^*

$$(2.9) \quad \langle \mathbf{J} \cdot \mathbf{E} \rangle = \rho^* \mathbf{J}_0 \cdot \mathbf{J}_0, \quad \mathbf{J} = \mathbf{J}_f + \mathbf{J}_0, \quad \langle \mathbf{J} \rangle = \mathbf{J}_0 = J_0 \mathbf{e}_k.$$

The resolvent formulas for the current density are analogous to equation (2.6) [26],

$$(2.10) \quad X_1 \mathbf{J} = t(tI - X_1 \Upsilon X_1)^{-1} X_1 \mathbf{J}_0, \quad X_2 \mathbf{J} = s(sI - X_2 \Upsilon X_2)^{-1} X_2 \mathbf{J}_0.$$

Analogous to equation (2.5), Stieltjes integral representations for the ρ_{jk}^* are given by [26]

$$(2.11) \quad H_{jk}(t) = 1 - \sigma_2 \rho_{jk}^* = \langle (tI - X_1 \Upsilon X_1)^{-1} X_1 \mathbf{e}_j \cdot \mathbf{e}_k \rangle = \int_0^1 \frac{d\kappa_{jk}(\lambda)}{t - \lambda}, \quad t = \frac{1}{1 - \sigma_1/\sigma_2}.$$

These integral representations yields rigorous *forward bounds* for the effective parameters of composites, given partial information on the microgeometry via the μ^n [3, 21, 14, 4]. One can also use the integral representations to obtain *inverse bounds*, allowing one to use data about the electromagnetic response of a sample, for example, to bound its structural parameters, such as the mean orientation angle of the crystallites [19, 20, 8, 6, 29, 5, 7, 9, 13].

3. STIELTJES INTEGRALS FOR BULK TRANSPORT COEFFICIENTS FOR DISCRETE MEDIA

In this section we adapt the discrete matrix analysis framework developed in [23] that describes effective transport in discrete two-component composite materials, such as a random resistor network, to formulate a mathematical framework that provides discrete, matrix analysis versions of the results reviewed in Section 2. We show that a discretization of the operators $X_1 \Gamma X_1$ and $X_1 \Upsilon X_1$, for example, lead to real-symmetric *random matrices*. Here, Γ and Υ are (non-random) projection matrices which depend only on the lattice topology and boundary conditions, and X_1 is a (random) projection matrix which determines the crystallite arrangement and orientation angles of the polycrystalline material.

In Section 3.1, we prove the existence of transport fields \mathbf{E} and \mathbf{J} satisfying discrete forms of the following systems of equations

$$(3.1) \quad \nabla \times \mathbf{E} = 0, \quad \nabla \cdot \mathbf{J} = 0, \quad \mathbf{J} = \sigma \mathbf{E}, \quad \mathbf{E} = \mathbf{E}_0 + \mathbf{E}_f, \quad \langle \mathbf{E} \rangle = \mathbf{E}_0,$$

$$(3.2) \quad \nabla \times \mathbf{E} = 0, \quad \nabla \cdot \mathbf{J} = 0, \quad \mathbf{E} = \rho \mathbf{J}, \quad \mathbf{J} = \mathbf{J}_0 + \mathbf{J}_f, \quad \langle \mathbf{J} \rangle = \mathbf{J}_0.$$

In Section 3.2, we solve these systems of equations by deriving resolvent representations for $X_i \mathbf{E}$ and $X_i \mathbf{J}$, $i = 1, 2$, in (2.6) and (2.10), with $\mathbf{E} = X_1 \mathbf{E} + X_2 \mathbf{E}$ and $\mathbf{J} = X_1 \mathbf{J} + X_2 \mathbf{J}$, in terms of the real-symmetric matrices $X_i \Gamma X_i$ and $X_i \Upsilon X_i$, $i = 1, 2$. We show that these resolvent representations have summation formulas given explicitly in terms of the real eigenvalues and orthonormal eigenvectors of the real-symmetric matrices $X_1 \Gamma X_1$ and $X_1 \Upsilon X_1$

$$(3.3) \quad X_1 \mathbf{E} = s E_0 \sum_j \frac{(\mathbf{w}_i \cdot X_1 \hat{\mathbf{e}}_k)}{s - \lambda_i} \mathbf{w}_i, \quad X_1 \mathbf{J} = t \mathbf{J}_0 \sum_i \frac{(\tilde{\mathbf{w}}_i \cdot X_1 \hat{\mathbf{e}}_k)}{t - \tilde{\lambda}_i} \tilde{\mathbf{w}}_i,$$

where the $(\lambda_i, \mathbf{w}_i)$ and $(\tilde{\lambda}_i, \tilde{\mathbf{w}}_i)$ are the eigenvalues and eigenvectors of the matrices $X_1 \Gamma X_1$ and $X_1 \Upsilon X_1$, respectively.

In Section 4, we show that the integrals in equations (2.5) and (2.11), for example, also have summation formulas [23],

$$(3.4) \quad F_{kk}(s) = \sum_i \left\langle \frac{m_i}{s - \lambda_i} \right\rangle, \quad m_i = |\mathbf{w}_i \cdot X_1 \hat{\mathbf{e}}_k|^2, \quad H_{kk}(t) = \sum_i \left\langle \frac{\tilde{m}_i}{t - \tilde{\lambda}_i} \right\rangle, \quad \tilde{m}_i = |\tilde{\mathbf{w}}_i \cdot X_1 \hat{\mathbf{e}}_k|^2,$$

where $\hat{\mathbf{e}}_k$ plays the role of a standard basis vector on the lattice. Then the discrete spectral measure μ_{kk} , for example, is given in terms of the eigenvalues λ_i and orthonormal eigenvectors \mathbf{w}_i of the matrix $X_1 \Gamma X_1$ [23],

$$(3.5) \quad \mu(d\lambda) = \langle Q(d\lambda) \hat{\mathbf{e}}_k \cdot \hat{\mathbf{e}}_k \rangle, \quad Q(d\lambda) = \sum_i \delta_{\lambda_i}(d\lambda) X_1 Q_i, \quad Q_i = \mathbf{w}_i \mathbf{w}_i^T.$$

Here, $Q(d\lambda)$ is the projection valued measure associated with the matrix $X_1 \Gamma X_1$, $\delta_{\lambda_i}(d\lambda)$ is the delta measure centered at λ_i , and the matrix $Q_i = \mathbf{w}_i \mathbf{w}_i^T$ is a projection onto the eigenspace spanned by \mathbf{w}_i [23].

3.1. Existence of transport fields for discrete media. In this section, we prove that there exists transport fields \mathbf{E} and \mathbf{J} that satisfy discrete versions of equations (3.1) and (3.2). Specifically, in Theorem 3.2, we prove the existence of an electric field \mathbf{E} satisfying a discrete version of the system of equations in (3.1). In Corollary 3.1, we prove that there exists a current field \mathbf{J} satisfying a discrete version of the system of equations in (3.2).

Towards this goal, we follow [17] and consider finite difference representations of the partial differential operators $\partial_i \rightarrow C_i$, $i = 1 \dots, d$, where d denotes dimension. The matrices C_i depend on boundary conditions which, without loss of generality, we take to be periodic boundary conditions. Denote the matrix

representation of the gradient operator ∇ (using Matlab vertical block notation) by $\nabla = [C_1; \dots; C_d]$. The discretization of the divergence operator is given by $-\nabla^T$ and the discrete curl operator $\nabla \times$ is given by [17]

$$(3.6) \quad C = \begin{bmatrix} O & -C_3 & C_2 \\ C_3 & O & -C_1 \\ -C_2 & C_1 & O \end{bmatrix} \text{ for 3D,} \\ C = [-C_2, C_1] \text{ for 2D.}$$

The operators C_i , $i = 1, 2, 3$, in (3.6) are normal and commute with each other [17],

$$(3.7) \quad C_i^T C_j = C_j C_i^T \text{ and } C_i C_j = C_j C_i, \text{ for } i, j = 1, 2, 3.$$

We now summarize some useful identities relating the discrete representations of the gradient, divergence, and curl operators which follow from these properties of the matrices C_i [17],

$$(3.8) \quad \begin{aligned} \Delta &= \nabla \cdot \nabla \rightarrow -\nabla^T \nabla, \\ \Delta &= \text{diag}(\Delta, \dots, \Delta) \rightarrow I_d \otimes (\nabla^T \nabla), \\ \nabla \times \nabla \times &\rightarrow C^T C, \\ \nabla \times \nabla \times &= \nabla(\nabla \cdot) - \Delta \rightarrow -\nabla \nabla^T + I_d \otimes (\nabla^T \nabla), \\ \nabla \cdot (\nabla \times) &\rightarrow -\nabla^T C^T = 0, \\ \nabla \times \nabla &\rightarrow C \nabla = 0, \end{aligned}$$

where \otimes denotes the Kronecker product. The last two identities $\nabla^T C^T = 0$ and $C \nabla = 0$ in equation (3.8) indicate that

$$(3.9) \quad \mathcal{R}(C^T) \subseteq \mathcal{K}(\nabla^T), \quad \mathcal{R}(\nabla) \subseteq \mathcal{K}(C)$$

Consequently, the discrete form of the system of equations in (3.1) and the energy constraint in (2.3) is

$$(3.10) \quad C \mathbf{E} = 0, \quad -\nabla^T \mathbf{J} = 0, \quad \mathbf{J} = \epsilon \mathbf{E}, \quad \mathbf{E} = \mathbf{E}_f + \mathbf{E}_0, \quad C \mathbf{E}_f = 0, \quad \langle \mathbf{J} \cdot \mathbf{E}_f \rangle = 0, \quad \langle \mathbf{E}_f \rangle = 0,$$

where in this finite size discrete setting, $\langle \cdot \rangle$ denotes volume average followed by ensemble average [23, 25]. To set notation, denote by $\mathcal{R}(B)$ and $\mathcal{K}(B)$ the range and kernel (null space) of a matrix B , respectively [16]. Therefore, we seek to prove that there exists a vector \mathbf{E} satisfying $\mathbf{E} \in \mathcal{K}(C)$ such that $\mathbf{E} = \mathbf{E}_f + \mathbf{E}_0$, where $\mathbf{E}_f \in \mathcal{K}(C)$ and $\langle \mathbf{E}_f \rangle = 0$ with $\mathbf{E}_0 \in \mathcal{K}(C)$, so $\langle \mathbf{E} \rangle = \mathbf{E}_0$. Moreover, we seek to find a vector $\mathbf{J} \in \mathcal{K}(\nabla^T)$ satisfying $\mathbf{J} = \epsilon \mathbf{E}$ and $\langle \mathbf{J} \cdot \mathbf{E}_f \rangle = 0$ and $\mathbf{J}_0 \in \mathcal{K}(\nabla^T)$. Given the formulas in equation (3.9), we focus on finding ‘‘potentials’’ φ and ψ such that $\mathbf{E}_f = \nabla \varphi$ and $\mathbf{J}_f = C^T \psi$.

The last two identities (3.8) provide a relationship between rank and kernel of the operators C , ∇ , and their transposes. The fundamental theorem of linear algebra [16] provides a relationship between the range of a matrix A and the kernel of its transpose A^T , which will be useful later in this section.

Theorem 3.1 (Fundamental theorem of linear algebra). *Let A be a real valued matrix of size $m \times n$ then*

$$(3.11) \quad \mathbb{R}^m = \mathcal{R}(A) \oplus \mathcal{K}(A^T), \quad \mathbb{R}^n = \mathcal{R}(A^T) \oplus \mathcal{K}(A),$$

where \oplus indicates $\mathcal{R}(A)$ is orthogonal to $\mathcal{K}(A^T)$, i.e., $\mathcal{R}(A) \perp \mathcal{K}(A^T)$, for example.

Applying Theorem 3.1 to the matrices ∇ and C^T indicates that $\mathbb{R}^m = \mathcal{R}(\nabla) \oplus \mathcal{K}(\nabla^T)$ and $\mathbb{R}^m = \mathcal{R}(C^T) \oplus \mathcal{K}(C)$. Therefore, from equation (3.9) we have that divergence-free fields are orthogonal to gradients (curl-free fields) and curl-free fields are orthogonal to $\mathcal{R}(C^T)$ (divergence-free fields). This is a discrete version of the Helmholtz Theorem, which states that curl-free and divergence-free fields (or, in other words, the gradient and cycle spaces) are mutually orthogonal. This also establishes the important relationship

$$(3.12) \quad \mathcal{R}(C^T) \perp \mathcal{R}(\nabla).$$

Orthogonal bases can be given for each of the mutually orthogonal spaces in equation (3.11) through the singular value decomposition (SVD) [16] of a matrix $A = U \Sigma V^T$, which also provides important information relating the matrices C , ∇ , etc. Here U and V are orthogonal matrices of size $m \times m$ and $n \times n$ satisfying $U^T U = U U^T = I_m$ and $V^T V = V V^T = I_n$, where I_m is the identity matrix of size m . Moreover, Σ is a diagonal matrix of size $m \times n$ with diagonal components consisting of the positive *singular values* ν_i ,

$i = 1, \dots, n$, of the matrix A satisfying $\nu_1 \geq \nu_2 \geq \dots \geq \nu_\rho > 0$ and $\nu_{\rho+1} = \nu_{\rho+2} = \dots = \nu_n = 0$, where ρ is the rank of A . Writing the matrix Σ in block form we have

$$(3.13) \quad \Sigma = \begin{bmatrix} \Sigma_1 & O_1 \\ O_1^T & O_2 \\ O_3 & O_4 \end{bmatrix},$$

where Σ_1 is a diagonal matrix of size $\rho \times \rho$ with diagonal consisting of the strictly positive singular values, O_1 and O_2 , are matrices of zeros of size $\rho \times (n - \rho)$ and $(n - \rho) \times (n - \rho)$, and the bottom block of zeros $[O_3, O_4]$ is of size $(m - n) \times n$.

Write the matrices U and V in block form as $U = [U_1, U_0, U_2]$ and $V = [V_1, V_0]$, where U_1 and V_1 are the columns of U and V corresponding to the strictly positive singular values in Σ_1 , U_0 and V_0 correspond to the the singular values with value zero, $\nu_i = 0$, and U_2 corresponds to the bottom block of zeros $[O_3, O_4]$ in Σ . Taking in account all the blocks of zeros in Σ , we can write $A = U_1 \Sigma_1 V_1^T$. We now state a well known fact about the SVD of the matrix A [16].

$$(3.14) \quad \mathcal{R}(A) = \text{Col}(U_1), \quad \mathcal{K}(A) = \text{Col}(V_0), \quad \mathcal{R}(A^T) = \text{Col}(V_1), \quad \mathcal{K}(A^T) = \text{Col}([U_0, U_2]),$$

where $\text{Col}(B)$ denotes the column space of the matrix B , i.e., the space spanned by the columns of B .

Applying the SVD to the matrices $\nabla = U^\times \Sigma^\times [V^\times]^T$ and $C^T = U^\bullet \Sigma^\bullet [V^\bullet]^T$ and using the orthogonality of the columns of the matrices U_1 and V_1 and the invertibility of Σ_1 , from $C\nabla = 0$ in (3.8) we have $[U^\bullet]^T U^\times = 0$, and similarly $\nabla^T C^T = 0$ implies $[U^\times]^T U^\bullet = 0$. The formula $[U^\bullet]^T U^\times = 0$ is a restatement of equation (3.12). Writing $U^\times = [U_1^\times, U_0^\times, U_2^\times]$ and $U^\bullet = [U_1^\bullet, U_0^\bullet, U_2^\bullet]$ we have established that $\mathcal{R}(\nabla) = \text{Col}(U_1^\times)$, $\mathcal{R}(C^T) \subseteq \mathcal{K}(\nabla^T) = \text{Col}([U_0^\times, U_2^\times])$. Also, since $\mathcal{R}(C^T) = \text{Col}(U_1^\bullet)$ and $\mathcal{R}(C^T) \perp \mathcal{R}(\nabla)$, we can write

$$(3.15) \quad U^\times = [U_1^\times, U_0^{\times\bullet}, U_1^\bullet], \quad U^\bullet = [U_1^\bullet, U_0^{\times\bullet}, U_1^\times],$$

where the columns of $U_0^{\times\bullet}$ are orthogonal to both the $\mathcal{R}(C^T)$ and the $\mathcal{R}(\nabla)$. Since $U^\times [U^\times]^T = I_m$ we have the *resolution of the identity*

$$(3.16) \quad \Gamma_\times + \Gamma_0 + \Gamma_\bullet = I_m, \quad \Gamma_\times = U_1^\times [U_1^\times]^T, \quad \Gamma_\bullet = U_1^\bullet [U_1^\bullet]^T, \quad \Gamma_0 = U_0^{\times\bullet} [U_0^{\times\bullet}]^T,$$

where Γ_\times , Γ_\bullet , and Γ_0 , are mutually orthogonal projection matrices onto $\mathcal{R}(\nabla)$, $\mathcal{R}(C^T)$ and the orthogonal complement of $\mathcal{R}(\nabla) \cup \mathcal{R}(C^T)$. We are now ready to state the main result of this section as the following theorem.

Theorem 3.2. *Let the electric and current fields \mathbf{E} and \mathbf{J} satisfy*

$$(3.17) \quad C\mathbf{E} = 0, \quad -\nabla^T \mathbf{J} = 0, \quad \mathbf{J} = \epsilon \mathbf{E}.$$

Then, there exists a ‘‘potential’’ φ and vector \mathbf{E}_0 such that $\mathbf{E} = \mathbf{E}_f + \mathbf{E}_0$, where $\mathbf{E}_f = \nabla\varphi$, $C\mathbf{E}_f = 0$, $\langle \mathbf{J}, \mathbf{E}_f \rangle = 0$, $\langle \mathbf{E}_f \rangle = 0$, and $I_d \otimes (\nabla^T \nabla) \mathbf{E}_0 = 0$, thus \mathbf{E}_0 is an arbitrary constant.

Proof. Let \mathbf{E} be the solution to equation (3.17). From the resolution of the identity in equation (3.16) we have $\mathbf{E} = (\Gamma_\times + \Gamma_0 + \Gamma_\bullet)\mathbf{E}$. Since Γ_\bullet projects onto the $\mathcal{R}(C^T)$, $\mathbb{R}^m = \mathcal{R}(C^T) \oplus \mathcal{K}(C)$, and $\mathbf{E} \in \mathcal{K}(C)$ we have $\Gamma_\bullet \mathbf{E} = 0$. Defining $\mathbf{E}_f = \Gamma_\times \mathbf{E}$, since $U_1^\times = \nabla V_1^\times [\Sigma_1^\times]^{-1}$, we can write $\mathbf{E}_f = \nabla\varphi$, where $\varphi = V_1^\times [\Sigma_1^\times]^{-1} [U_1^\times]^T \mathbf{E}$.

Define $\mathbf{E}_0 = \Gamma_0 \mathbf{E}$. Since $\Gamma_\times \mathbf{E}_0 = 0$, Γ_\times is a projection onto $\mathcal{R}(\nabla)$, and $\mathbb{R}^m = \mathcal{R}(\nabla) \oplus \mathcal{K}(\nabla^T)$, we have $\mathbf{E}_0 \in \mathcal{K}(\nabla^T)$. Similarly, since $\Gamma_\bullet \mathbf{E}_0 = 0$, Γ_\bullet is a projection onto $\mathcal{R}(C^T)$, and $\mathbb{R}^m = \mathcal{R}(C^T) \oplus \mathcal{K}(C)$, we have $\mathbf{E}_0 \in \mathcal{K}(C)$. Since $\mathbf{E}_0 \in \mathcal{K}(C) \cap \mathcal{K}(\nabla^T)$ we have from (3.8) that

$$(3.18) \quad 0 = C^T C \mathbf{E}_0 = (-\nabla \nabla^T + I_d \otimes (\nabla^T \nabla)) \mathbf{E}_0 = I_d \otimes (\nabla^T \nabla) \mathbf{E}_0,$$

which determines \mathbf{E}_0 and establishes that the solution to (3.17) can be written as $\mathbf{E} = \nabla\varphi + \mathbf{E}_0$. Equation (3.18) implies that each dimensional component $(\mathbf{E}_0)_i$, $i = 1, \dots, d$, which is a vector in this discrete setting [23], satisfies $\nabla^T \nabla (\mathbf{E}_0)_i$. Therefore,

$$(3.19) \quad 0 = \nabla^T \nabla (\mathbf{E}_0)_i \cdot (\mathbf{E}_0)_i = \nabla (\mathbf{E}_0)_i \cdot \nabla (\mathbf{E}_0)_i = \|\nabla (\mathbf{E}_0)_i\|^2,$$

where $\|\cdot\|$ denotes ℓ^2 -norm. It follows that $(\mathbf{E}_0)_i$ is constant for each $i = 1, \dots, d$, hence \mathbf{E}_0 is an arbitrary constant vector.

From $\mathcal{R}(\nabla) \subseteq \mathcal{K}(C)$ in equation (3.9) and $\mathbf{E}_f = \nabla\varphi$ we have $C\mathbf{E}_f = C\nabla\varphi = 0$. We also have from $\nabla^T \mathbf{J} = 0$ that $\mathbf{J} \cdot \mathbf{E}_f = \mathbf{J} \cdot \nabla\varphi = \nabla^T \mathbf{J} \cdot \varphi = 0$. Finally, the volume average of $\nabla\varphi$ is a telescoping sum, so $\langle \mathbf{E}_f \rangle = 0$. This concludes our proof of the theorem. \square

Corollary 3.1. *Let the electric and current fields \mathbf{E} and \mathbf{J} satisfy*

$$(3.20) \quad C\mathbf{E} = 0, \quad -\nabla^T \mathbf{J} = 0, \quad \mathbf{E} = \rho \mathbf{J}.$$

Then, there exists a “potential” ψ and vector \mathbf{J}_0 such that $\mathbf{J} = \mathbf{J}_f + \mathbf{J}_0$, where $\mathbf{J}_f = C^T \psi$, $\nabla^T \mathbf{J}_f = 0$, $\langle \mathbf{J}_f \cdot \mathbf{E} \rangle = 0$, $\langle \mathbf{J}_f \rangle = 0$, and $I_d \otimes (\nabla^T \nabla) \mathbf{J}_0 = 0$, thus \mathbf{J}_0 is an arbitrary constant.

Proof. Let \mathbf{J} be the solution to equation (3.20). From the resolution of the identity in equation (3.16) we have $\mathbf{J} = (\Gamma_\times + \Gamma_0 + \Gamma_\bullet) \mathbf{J}$. Since Γ_\times projects onto the $\mathcal{R}(\nabla)$, $\mathbb{R}^m = \mathcal{R}(\nabla) \oplus \mathcal{K}(\nabla^T)$, and $\mathbf{J} \in \mathcal{K}(\nabla^T)$ we have $\Gamma_\times \mathbf{J} = 0$. Defining $\mathbf{J}_f = \Gamma_\bullet \mathbf{J}$, since $U_1^\bullet = C^T V_1^\bullet [\Sigma_1^\bullet]^{-1}$, we can write $\mathbf{J}_f = C^T \psi$, where $\psi = V_1^\bullet [\Sigma_1^\bullet]^{-1} [U_1^\bullet]^T \mathbf{J}$. Define $\mathbf{J}_0 = \Gamma_0 \mathbf{J}$. Exactly the same as in the proof of Theorem 3.2, we have $I_d \otimes (\nabla^T \nabla) \mathbf{J}_0 = 0$, which determines \mathbf{J}_0 to be an arbitrary constant vector and establishes that the solution to (3.20) can be written as $\mathbf{J} = C^T \psi + \mathbf{J}_0$. From $\mathcal{R}(C^T) \subseteq \mathcal{K}(\nabla^T)$ in equation (3.9) and $\mathbf{J}_f = C^T \psi$ we have $\nabla^T \mathbf{J}_f = \nabla^T C^T \psi = 0$. Exactly the same as in the proof of Theorem 3.2, we also have $\mathbf{J}_f \cdot \mathbf{E} = 0$ and $\langle \mathbf{J}_f \rangle = 0$. This concludes our proof of the theorem. \square

We end this section by noting that in the full rank setting, where Σ has all strictly positive singular values, so $\Sigma_1 = \Sigma$, then

$$(3.21) \quad \Gamma_\times = \nabla (\nabla^T \nabla)^{-1} \nabla^T, \quad \Gamma_\bullet = C^T (C C^T)^{-1} C.$$

The original formulations of this mathematical framework was given in terms of these projection matrices, or continuum generalizations [14, 23]. The formulation given in this section generalizes the discrete setting to cases where the matrix gradient is rank deficient, such as the case of periodic boundary conditions. To simplify notation to that used in [26], for the remainder of the manuscript we will denote $\Gamma = \Gamma_\times$ and $\Upsilon = \Gamma_\bullet$.

3.2. Resolvent representations for transport fields. In this section, we utilize the results of Theorem 3.2 to explicitly solve the system of equations in (3.17) for \mathbf{E} . We accomplish this by deriving resolvent formulas for the fields $X_i \mathbf{E}$, $i = 1, 2$, in (2.6) in terms of the real-symmetric matrices $X_i \Gamma X_i$, $i = 1, 2$. The electric field can then be constructed using $\mathbf{E} = X_1 \mathbf{E} + X_2 \mathbf{E}$ and the current density can be constructed using $\mathbf{J} = \sigma_1 X_1 \mathbf{E} + \sigma_2 X_2 \mathbf{E}$. Similarly, we utilize the results of Corollary 3.1 to explicitly solve the system of equations in (3.20) for \mathbf{J} by deriving resolvent formulas for the fields $X_i \mathbf{J}$, $i = 1, 2$, in (2.10) in terms of the real-symmetric matrices $X_i \Upsilon X_i$, $i = 1, 2$. The current field can then be constructed using $\mathbf{J} = X_1 \mathbf{J} + X_2 \mathbf{J}$ and the electric field can be constructed using $\mathbf{E} = \sigma_1^{-1} X_1 \mathbf{J} + \sigma_2^{-1} X_2 \mathbf{J}$. These resolvent formulas provide eigenvector expansions for the physical fields \mathbf{E} and \mathbf{J} , which can be used to numerically calculate them, which we do in Section 5.

We provide a detailed derivation of the resolvent formula shown in (2.6) for the setting where the gradient matrix ∇ is full rank and rank deficient. Other resolvent formulas are obtained in an analogous manner. From Theorem 3.2 and equation (3.17) we can apply the operator $\nabla (\nabla^T \nabla)^{-1}$ to the formula $-\nabla^T \mathbf{J} = 0$ to obtain $\Gamma \mathbf{J} = 0$, where $\Gamma = \nabla (\nabla^T \nabla)^{-1} \nabla^T$ is a projection onto $\mathcal{R}(\nabla)$. In the full rank setting, the SVD for $\nabla = U_1 \Sigma_1 V_1^T$, where all singular values have strictly positive value. In this case, the square $n \times n$ diagonal matrix Σ_1 is invertible, U_1 is an $m \times n$ with left inverse satisfying $U_1^T U_1 = I_m$, and V_1 is an $n \times n$ unitary matrix satisfying $V_1 V_1^T = V_1^T V_1 = I_n$ [16]. Using these matrix properties, we have $\Gamma = \nabla (\nabla^T \nabla)^{-1} \nabla^T = U_1 U_1^T$ [24].

When ∇ is rank deficient, one or more of the singular values have value 0. We can still write $\nabla = U_1 \Sigma_1 V_1^T$ [16, 24]. However, now the diagonal matrix Σ_1 is smaller than in the full rank setting but it is still invertible, and both the matrices U_1 and V_1 just have left inverses satisfying $V_1^T V_1 = I_n$ and $U_1^T U_1 = I_m$ [16, 24]. The key observation is that we can use these matrix properties to again write $-\nabla^T \mathbf{J} = 0$ as $\Gamma \mathbf{J} = 0$ where we define $\Gamma = U_1 U_1^T$, and Γ is still a projection on to $\mathcal{R}(\nabla)$ [16, 24].

Writing equation (2.1) as $\sigma = \sigma_2 (1 - X_1/s)$, using the results of Theorem 3.2 to write $\Gamma \mathbf{E}_f = \mathbf{E}_f$, $\Gamma \mathbf{E}_0 = 0$, and $\mathbf{J} = \sigma_2 (1 - X_1/s) (\mathbf{E}_f + \mathbf{E}_0)$, the formula $\Gamma \mathbf{J} = 0$ can be written as $\mathbf{E}_f - \Gamma X_1 \mathbf{E}_f/s = 0$ [23]. Adding \mathbf{E}_0 to both sides then applying X_1 to the left of both sides, using $X_1^2 = X_1$, and rearranging yields

$$(3.22) \quad (sI - X_1 \Gamma X_1) X_1 \mathbf{E} = s X_1 \mathbf{E}_0,$$

which is equivalent to equation (2.6). In a similar fashion one finds

$$(3.23) \quad \begin{aligned} X_1 \mathbf{E} &= s(sI - X_1 \Gamma X_1)^{-1} X_1 \mathbf{E}_0, \\ X_2 \mathbf{E} &= t(tI - X_2 \Gamma X_2)^{-1} X_2 \mathbf{E}_0, \\ X_1 \mathbf{J} &= t(tI - X_1 \Upsilon X_1)^{-1} X_1 \mathbf{J}_0, \\ X_2 \mathbf{J} &= s(sI - X_2 \Upsilon X_2)^{-1} X_2 \mathbf{J}_0. \end{aligned}$$

These formulas determine the physical fields \mathbf{E} and \mathbf{J} via $\mathbf{E} = X_1 \mathbf{E} + X_2 \mathbf{E}$ and $\mathbf{J} = \sigma_1 X_1 \mathbf{E} + \sigma_2 X_2 \mathbf{E}$.

4. STIELTJES INTEGRALS FOR BULK TRANSPORT COEFFICIENTS

We start this section with a high level description of discrete Stieltjes integral representations for the bulk transport coefficients of uniaxial polycrystalline materials. We then utilize properties of the projection matrices in $X_1 \Gamma X_1$, for example, to provide a more detailed analysis and develop a projection method to show that the spectral measure can be computed by much smaller matrices, which leads to a more efficient and stable numerical algorithm for the computation of bulk transport coefficients and physical fields.

Using the the resolvent formula for $X_1 \mathbf{E}$ in equation (2.6), the energy functional in equation (2.4), $\langle \mathbf{E}_f \rangle = 0$, and $\mathbf{E} = E_0 \hat{\mathbf{e}}_k$ we have

$$(4.1) \quad \langle \mathbf{J} \cdot \mathbf{E}_0 \rangle = \sigma_2 E_0^2 (1 - \langle X_1 \mathbf{E} \cdot X_1 \hat{\mathbf{e}}_k \rangle / s) = \sigma_2 E_0^2 (1 - \langle (sI - X_1 \Gamma X_1)^{-1} X_1 \hat{\mathbf{e}}_k \cdot X_1 \hat{\mathbf{e}}_k \rangle),$$

where $\hat{\mathbf{e}}_k$ is the discretized version of the standard basis vector \mathbf{e}_k [23]. Since the matrix $X_1 \Gamma X_1$ is real-symmetric, it can be written [16] as $X_1 \Gamma X_1 = W \Lambda W^T$, where the Λ is a diagonal matrix with diagonal entries comprised of the real eigenvalues λ_i of the matrix $X_1 \Gamma X_1$ and the columns of W are composed of the orthonormal eigenvectors \mathbf{w}_i of the matrix, satisfying $W W^T = W^T W = I$. Therefore, we have [23]

$$(4.2) \quad F_{kk}(s) = \langle (sI - X_1 \Gamma X_1)^{-1} X_1 \hat{\mathbf{e}}_k \cdot X_1 \hat{\mathbf{e}}_k \rangle = \langle (sI - \Lambda)^{-1} W^T X_1 \hat{\mathbf{e}}_k \cdot W^T X_1 \hat{\mathbf{e}}_k \rangle,$$

which can be written as the summation formula for $F_{kk}(s)$ in equation (3.4).

The following theorem is a refinement of this result and provides a rigorous mathematical formulation of integral representations for the effective parameters for finite lattice approximations of random uniaxial polycrystalline media.

Theorem 4.1. *For each $\omega \in \Omega$, let $M(\omega) = W(\omega) \Lambda(\omega) W(\omega)$ be the eigenvalue decomposition of the real-symmetric matrix $M(\omega) = X_1(\omega) \Gamma X_1(\omega)$. Here, the columns of the matrix $W(\omega)$ consist of the orthonormal eigenvectors $\tilde{\mathbf{w}}_i(\omega)$, $i = 1, \dots, N$, of $M(\omega)$ and the diagonal matrix $\Lambda(\omega) = \text{diag}(\lambda_1(\omega), \dots, \lambda_N(\omega))$ involves its eigenvalues $\lambda_i(\omega)$. Denote $Q_i = \tilde{\mathbf{w}}_i \tilde{\mathbf{w}}_i^T$ the projection matrix onto the eigen-space spanned by $\tilde{\mathbf{w}}_i$. The electric field $\mathbf{E}(\omega)$ satisfies $\mathbf{E}(\omega) = \mathbf{E}_0 + \mathbf{E}_f(\omega)$, with $\mathbf{E}_0 = \langle \mathbf{E}(\omega) \rangle$ and $\Gamma \mathbf{E}(\omega) = \mathbf{E}_f(\omega)$, and the effective complex permittivity tensor ϵ^* has components ϵ_{jk}^* , $j, k = 1, \dots, d$, which satisfy*

$$(4.3) \quad \epsilon_{jk}^* = \epsilon_2 (\delta_{jk} - F_{jk}(s)), \quad F_{jk}(s) = \int_0^1 \frac{d\mu_{jk}(\lambda)}{s - \lambda}, \quad d\mu_{jk}(\lambda) = \sum_{i=1}^N \langle \delta_{\lambda_i} (d\lambda) X_1 Q_i \hat{\mathbf{e}}_j \cdot \hat{\mathbf{e}}_k \rangle.$$

Theorem 4.1 holds for both of the settings where the matrix gradient is full rank or rank deficient. To numerically compute the μ_{jk} a non-standard generalization of the spectral theorem for matrices is required, due to the projective nature of the matrices X_1 and Γ [23]. In particular, we develop a *projection method* that shows the spectral measure μ_{jk} in (4.3) depends only on the eigenvalues and eigenvectors of the upper left $N_1 \times N_1$ block of the matrix $R \Gamma R^T$, where $N_1 = N/d$. These submatrices are smaller by a factor of d , which improves the efficiency and numerical computations of μ by a factor of d^3 [10, 28].

In this section we provide the proof for Theorem 4.1 and a projection method for a numerically efficient projection method for computation of spectral measures and effective parameters for uniaxial polycrystalline media. We will use the results from Section 3.1 but for notational simplicity we will use Γ instead of Γ_\times . Corollary 4.1 below follows immediately from the proof of Theorem 4.1 and the results of Section 3.1, which provides an integral representation for the effective resistivity $\boldsymbol{\rho}^*$ involving the matrix $X_2 \Gamma_\bullet X_2$ and is analogous to the representation of $\boldsymbol{\rho}^*$ for the two-component composite setting in [23].

From the close analogues of this polycrystalline setting with the two-component setting discussed in [26], the proof of this theorem is analogous to Theorem 2.1 in [23]. To shorten the theorem proof here, we will refer to [23] for some of the technical details. From Section 3.1 and the paragraph in [23] containing

equations (2.39) and (2.40), with χ_1 replaced by X_1 , we just need to prove that the functional $F_{jk}(s) = \langle (sI - X_1\Gamma X_1)^{-1} X_1 \hat{e}_j \cdot \hat{e}_k \rangle$ has the integral representation displayed in equation (4.3). In the process, we will also establish a projection method for the numerically efficient, rigorous computation of μ_{jk} . This projection method is summarized by equations (4.12)–(4.14) below.

In equations (4.1) and (4.2) we gave a brief description about how Stieltjes integral representations for the $F_{kk}(s)$ arise. We now give a more thorough analysis and pay close attention to the projective nature of the matrices X_1 and Γ . In [26] we defined the real-symmetric mutually orthogonal projection matrices X_i , $i = 1, 2$, in terms of the *spatially dependent* rotation matrix R and $C = \text{diag}(1, 0, \dots, 0)$, all matrices of size $d \times d$. The paragraph in [23] containing equations (2.28)–(2.30) describes how to bijectively map these $d \times d$ matrices to $N \times N$ matrices that are *not* spatially dependent, where $N = L^d d$. Under this mapping, R becomes a banded rotation matrix satisfying $R^T = R^{-1}$ and C becomes $C = \text{diag}(I_1, 0_1, \dots, 0_1)$, where I_1 and 0_1 are the identity and null matrices of size $N_1 = L^d$, and the vector e_1 is mapped to $\hat{e}_1 = (1, 1, \dots, 1, 0, 0, \dots, 0)$, with L^d ones in the first components and zeros in the rest of the components.

Writing $X_1\Gamma X_1 = R^T(CR\Gamma R^T C)R$ we have

$$(4.4) \quad \begin{aligned} X_1\Gamma X_1 &= R^T \begin{bmatrix} \Gamma_1 & 0_{12} \\ 0_{21} & 0_{22} \end{bmatrix} R = R^T \begin{bmatrix} W_1\Lambda_1 W_1^T & 0_{12} \\ 0_{21} & 0_{22} \end{bmatrix} R \\ &= R^T \begin{bmatrix} W_1 & 0_{12} \\ 0_{21} & I_2 \end{bmatrix} \begin{bmatrix} \Lambda_1 & 0_{12} \\ 0_{21} & 0_{22} \end{bmatrix} \begin{bmatrix} W_1^T & 0_{12} \\ 0_{21} & I_2 \end{bmatrix} R, \end{aligned}$$

where I_2 is the identity matrix of size $N_2 \times N_2$, with $N_2 = N - N_1 = L^d(d - 1)$, and 0_{ab} denotes a matrix of zeros of size $N_a \times N_b$, $a, b = 1, 2$. Moreover, Γ_1 is the $N_1 \times N_1$ upper left principal sub-matrix of $R\Gamma R^T$ and $\Gamma_1 = W_1\Lambda_1 W_1^T$ is its eigenvalue decomposition. As Γ_1 is a real-symmetric matrix, W_1 is an orthogonal matrix [16]. Also, since $R\Gamma R^T$ is a similarity transformation of a projection matrix and C is a projection matrix, Λ_1 is a diagonal matrix with entries $\lambda_i^1 \in [0, 1]$, $i = 1, \dots, N_1$, along its diagonal [16, 10]. Consequently, equation (4.4) implies that the eigenvalue decomposition of the matrix $X_1\Gamma X_1$ is given by

$$(4.5) \quad X_1\Gamma X_1 = W\Lambda W^T, \quad W = R^T \begin{bmatrix} W_1 & 0_{12} \\ 0_{21} & I_2 \end{bmatrix}, \quad \Lambda = \begin{bmatrix} \Lambda_1 & 0_{12} \\ 0_{21} & 0_{22} \end{bmatrix}.$$

Here, W is an orthogonal matrix satisfying $W^T W = W W^T = I$, I is the identity matrix on \mathbb{R}^N , and Λ is a diagonal matrix with entries $\lambda_i \in [0, 1]$, $i = 1, \dots, N$, along its diagonal.

The eigenvalue decomposition of the matrix $X_1\Gamma X_1$ in equation (4.5) demonstrates that its resolvent $(sI - X_1\Gamma X_1)^{-1}$ is well defined for all $s \in \mathbb{C} \setminus [0, 1]$. In particular, by the orthogonality of the matrix W , it has the following useful representation $(sI - X_1\Gamma X_1)^{-1} = W(sI - \Lambda)^{-1} W^T$, where $(sI - \Lambda)^{-1}$ is a diagonal matrix with entries $1/(s - \lambda_i)$ along its diagonal. This, in turn, implies that the functional $F_{jk}(s) = \langle (sI - X_1\Gamma X_1)^{-1} X_1 \hat{e}_j \cdot \hat{e}_k \rangle$ can be written as

$$(4.6) \quad F_{jk}(s) = \langle (sI - \Lambda)^{-1} [X_1 W]^T \hat{e}_j \cdot W^T \hat{e}_k \rangle.$$

Since $R^T = R^{-1}$ and $X_1 = R^T C R$, equation (4.5) implies that

$$(4.7) \quad X_1 W = R^T \begin{bmatrix} W_1 & 0_{12} \\ 0_{21} & 0_{22} \end{bmatrix} \implies X_1 \mathbf{w}_i = \begin{cases} \mathbf{w}_i, & \text{for } i = 1, \dots, N_1, \\ 0, & \text{otherwise.} \end{cases}$$

This and the formula for W in (4.5) imply that

$$(4.8) \quad [X_1 W]^T \hat{e}_j \cdot W^T \hat{e}_k = [X_1 W]^T \hat{e}_j \cdot [X_1 W]^T \hat{e}_k.$$

We are ready to provide the integral representation displayed in (4.3) for the functional $F_{jk}(s)$ in equation (4.6). Denote by $Q_i = \mathbf{w}_i \mathbf{w}_i^T$, $i = 1, \dots, N$, the symmetric, mutually orthogonal projection matrices, $Q_\ell Q_m = Q_\ell \delta_{\ell m}$, onto the eigen-spaces spanned by the orthonormal eigenvectors \mathbf{w}_i . Equation (4.7) implies that $X_1 Q_i = Q_i X_1 = X_1 Q_i X_1$, as $X_1 Q_i = Q_i$ for $i = 1, \dots, N_1$, $X_1 Q_i = 0$ otherwise, and X_1 is a symmetric matrix. These properties allow us to write the quadratic form $[X_1 W]^T \hat{e}_j \cdot [X_1 W]^T \hat{e}_k$ as

$$(4.9) \quad [X_1 W]^T \hat{e}_j \cdot [X_1 W]^T \hat{e}_k = W^T \hat{e}_j \cdot W^T \hat{e}_k = \sum_{i=1}^N (\mathbf{w}_i \cdot \hat{e}_j) (\mathbf{w}_i \cdot \hat{e}_k) = \sum_{i=1}^N Q_i \hat{e}_j \cdot \hat{e}_k = \sum_{i=1}^N X_1 Q_i \hat{e}_j \cdot \hat{e}_k.$$

This and equations (4.6) and (4.8) yield

$$(4.10) \quad F_{jk}(s) = \int_0^1 \frac{d\mu_{jk}(\lambda)}{s - \lambda}, \quad d\mu_{jk}(\lambda) = \sum_{i=1}^N \langle \delta_{\lambda_i}(d\lambda) X_1 Q_i \hat{e}_j \cdot \hat{e}_k \rangle.$$

This concludes our proof of Theorem 4.1

Corollary 4.1. *For each $\omega \in \Omega$, let $M(\omega) = W(\omega)\Lambda(\omega)W(\omega)$ be the eigenvalue decomposition of the real-symmetric matrix $M(\omega) = X_2(\omega)\Gamma_\bullet X_2(\omega)$. Here, the columns of the matrix $W(\omega)$ consist of the orthonormal eigenvectors $\tilde{\mathbf{w}}_i(\omega)$, $i = 1, \dots, N$, of $M(\omega)$ and the diagonal matrix $\Lambda(\omega) = \text{diag}(\lambda_1(\omega), \dots, \lambda_N(\omega))$ involves its eigenvalues $\lambda_i(\omega)$. Denote $Q_i = \tilde{\mathbf{w}}_i \tilde{\mathbf{w}}_i^T$ the projection matrix onto the eigen-space spanned by $\tilde{\mathbf{w}}_i$. The current field $\mathbf{J}(\omega)$ satisfies $\mathbf{J}(\omega) = \mathbf{J}_0 + \mathbf{J}_f(\omega)$, with $\mathbf{J}_0 = \langle \mathbf{J}(\omega) \rangle$ and $\Gamma_\bullet \mathbf{J}(\omega) = \mathbf{J}_f(\omega)$, and the effective complex resistivity tensor $\boldsymbol{\rho}^*$ has components ρ_{jk}^* , $j, k = 1, \dots, d$, which satisfy*

$$(4.11) \quad \rho_{jk}^* = \sigma_1^{-1}(\delta_{jk} - E_{jk}(s)), \quad E_{jk}(s) = \int_0^1 \frac{d\eta_{jk}(\lambda)}{s - \lambda}, \quad d\eta_{jk}(\lambda) = \sum_{i=1}^N \langle \delta_{\lambda_i}(d\lambda) X_2 Q_i \hat{e}_j \cdot \hat{e}_k \rangle.$$

4.1. Projection method. In this section we provide a formulation for a numerically efficient *projection method* for computation of spectral measures and effective parameters for uniaxial polycrystalline media. Note that the sum in equation (4.10) runs only over the index set $i = 1, \dots, N_1$, as equation (4.7) implies that the masses $X_1 Q_i \hat{e}_j \cdot \hat{e}_k$ of the measure μ_{jk} are zero for $i = N_1 + 1, \dots, N$. Denote by λ_i^1 and \mathbf{w}_i^1 , $i = 1, \dots, N_1$, the eigenvalues and eigenvectors of the $N_1 \times N_1$ matrix $\Gamma_1 = W_1 \Lambda_1 W_1^T$, defined in equation (4.4). Now, write

$$(4.12) \quad R\hat{e}_j = \begin{bmatrix} \hat{e}_j^{r_1} \\ \hat{e}_j^{r_2} \end{bmatrix},$$

where $\hat{e}_j^{r_1} \in \mathbb{R}^{N_1}$ and $\hat{e}_j^{r_2} \in \mathbb{R}^{N_2}$. Therefore, writing the matrix $X_1 W$ in equation (4.7) in block diagonal form, $X_1 W = R^T \text{diag}(W_1, 0_{22})$, we have that

$$(4.13) \quad [X_1 W]^T \hat{e}_j \cdot [X_1 W]^T \hat{e}_k = [\text{diag}(W_1^T, 0_{22}) R \hat{e}_j] \cdot [\text{diag}(W_1^T, 0_{22}) R \hat{e}_k] = [W_1^T \hat{e}_j^{r_1}] \cdot [W_1^T \hat{e}_k^{r_1}].$$

Denote by $Q_i^1 = \mathbf{w}_i^1 [\mathbf{w}_i^1]^T$, $i = 1, \dots, N_1$, the mutually orthogonal projection matrices, $Q_\ell^1 Q_m^1 = Q_\ell^1 \delta_{\ell m}$, onto the eigen-spaces spanned by the orthonormal eigenvectors \mathbf{w}_i^1 . Equations (4.6), (4.8), and (4.13) then yield

$$(4.14) \quad F_{jk}(s) = \langle (sI_1 - \Lambda_1)^{-1} [W_1^T \hat{e}_j^{r_1}] \cdot [W_1^T \hat{e}_k^{r_1}] \rangle = \left\langle \sum_{i=1}^{N_1} \frac{Q_i^1 \hat{e}_j^{r_1} \cdot \hat{e}_k^{r_1}}{s - \lambda_i^1} \right\rangle.$$

Equation (4.14) demonstrates that only the spectral information of the matrices W_1 and Λ_1 contribute to the functional representation for $F_{jk}(s)$ in (4.6) and its integral representation in (4.3). From a computational standpoint, this means that only the eigenvalues and eigenvectors of the $N_1 \times N_1$ matrix Γ_1 need to be computed in order to compute the spectral measures underlying the integral representations of the effective parameters for finite lattice systems. This is extremely cost effective as the numerical cost of finding all the eigenvalues and eigenvectors of a real-symmetric $N \times N$ matrix is $O(N^3)$ [10], so $N_1 = N/d$ implies the computational cost of the projection method is reduced by a factor of d^3 .

5. NUMERICAL RESULTS

In this section, we utilize Theorem 4.1 and the projection method of Section 4.1 to compute discrete, Stieltjes integral representations for the effective conductivity of two- and three-dimensional uniaxial polycrystalline media. We consider two-dimensional square polycrystalline media composed of a grid of randomly oriented square crystals as well as three-dimensional cubic media composed of stacked grids of randomly oriented cubic crystals. For simplicity, we will focus on the first diagonal component of the effective conductivity tensor and the underlying spectral measure μ_{11} . The values of the conductivities for each crystallite are taken to be $\sigma_1 = 51.0741 + i45.1602$ in the x -direction and $\sigma_2 = 3.07 + i0.0019$ in both y - and z -directions, so that $s \approx -0.034 + i0.032$.

We now discuss our numerical method for computing spectral measures and effective transport coefficients in this matrix setting. Consider a uniaxial polycrystalline medium consisting of randomly oriented crystallites indexed by $\omega \in \Omega$ and described by the matrix $X_1(\omega) = R^T(\omega)CR(\omega)$. In particular, for fixed $\omega \in \Omega$, the

measure $\mu_{kk}(\omega)$ is a weighted sum of δ -measures centered at the eigenvalues $\lambda_i(\omega)$ of $M(\omega)$, $i = 1, \dots, N$, with weights $[X_1(\omega)Q_i(\omega)\hat{e}_k] \cdot \hat{e}_k$ involving the eigenvectors $\mathbf{w}_i(\omega)$ of $M(\omega)$ via $Q_i = \mathbf{w}_i\mathbf{w}_i^T$. However, equation 4.7 implies that the measure weights $[X_1(\omega)Q_i(\omega)\hat{e}_k] \cdot \hat{e}_k$ are identically zero for $i = 1, \dots, N_0(\omega)$. This was used in equation (4.14) to show that the measure $\mu_{kk}(\omega)$ depends only on the eigenvalues $\lambda_i^1(\omega)$, $i = 1, \dots, N_1(\omega)$, and the eigenvectors $\mathbf{w}_i(\omega)$ of the principal sub-matrix $\Gamma_1(\omega)$ of $M(\omega)$, and that the measure weights can be expressed more explicitly as $Q_i^1(\omega)\hat{e}_k^{\pi_1} \cdot \hat{e}_k^{\pi_1}$ with $Q_i^1 = \mathbf{w}_i^1[\mathbf{w}_i^1]^T$. Consequently, for fixed $s \in \mathbb{C} \setminus [0, 1]$, the value of the effective complex conductivity $\sigma_{kk}^* = \sigma_2(1 - F_{kk}(s))$ of the medium can be obtained by computing $\lambda_i^1(\omega)$ and $\mathbf{w}_i^1(\omega)$ for all $i = 1, \dots, N_1(\omega)$ for each $\omega \in \Omega$. Since the computational cost of finding all the eigenvalues and eigenvectors of a $N \times N$ real-symmetric matrix is $O(N^3)$, this ‘‘projection method’’ makes the numerical computation of μ_{kk} and σ_{kk}^* more efficient by a factor of $1/d$.

For the randomly oriented polycrystalline media described above, the cardinality $|\Omega|$ of the sample space Ω of geometric configurations is infinite due to the continuous distribution that each crystallite orientation is sampled from. In our numerical computations, every crystallite orientation θ_j is sampled from $U([0, 2\pi])$ measured from the x -axis (in 2D) and from the z -axis (in 3D). For a given arrangement of crystallites, the orientation angles θ_j for each crystallite constitutes a single geometric configuration $\omega \in \Omega$. For each $\omega \in \Omega$, all of the eigenvalues and eigenvectors of the matrix $\Gamma_1(\omega)$ were computed using the MATLAB function *eig()* despite the streamlined projection method described previously. This is necessary in order to calculate the corresponding current density \mathbf{J} which is detailed below.

In order to visually determine the behavior of the function $\mu_{11}(\lambda) = \langle Q(\lambda)\hat{e}_1, \hat{e}_1 \rangle_1$ underlying the spectral measure μ_{11} for a given random polycrystalline geometry, we plot a histogram representation of $\mu_{11}(\lambda)$, called the *spectral function*, which we will also denote by $\mu_{11}(\lambda)$. In order to compute the spectral function $\mu_{11}(\lambda)$, the spectral interval $[0, 1]$ was divided into K sub-intervals I_k , $k = 1, \dots, K$, of equal length $1/K$. Next, for fixed k , we sum the discrete spectral measure weights $m_i = X_1Q_i\hat{e}_1 \cdot \hat{e}_1$ where i are the indices that correspond to each λ_i that is in the interval I_k . Averaging this sum over the total number of geometric configurations produces the value displayed in the spectral function over the interval I_k .

In Figure 1(a), we display the spectral measure weights m_i versus the associated eigenvalue λ_i for a single geometric configuration of a square grid (top row) consisting of 16 (4×4) square crystallites of length $L_c = 50$ and for a cubic grid (bottom row) consisting of 27 ($3 \times 3 \times 3$) cubic crystallites of length $L_c = 10$. Histogram representations of the measure weights (the spectral function) is displayed in Figure 1(b), where the top row represents a 3×3 grid of square crystallites with $L_c = 25$ and the bottom row represents a $4 \times 4 \times 4$ grid of cubic crystallites of length $L_c = 4$. The measure weights are averaged over 2000 geometric configurations, resulting in smooth spectral functions. We reduce the length L_c for these histogram representations with respect to Figure 1(a) due to the large number of geometric configurations and requisite computations required.

Figure 1(c) displays the current density $\mathbf{J} = \sigma\mathbf{E} = \sigma_1X_1\mathbf{E} + \sigma_2X_2\mathbf{E}$ with \mathbf{E}_0 taken to be \hat{e}_2 (oriented along the y axis). The components $X_1\mathbf{E}$ and $X_2\mathbf{E}$ are computing using Equation (3.3). The geometric configuration and orientation angles θ_j are identical to the configuration and angles taken in Figure 1(a). The orientation angles $\theta \in [-\pi, \pi]$ of each crystallite are given in Figure 1(d).

6. CONCLUSIONS

We formulated a rigorous mathematical framework that provides Stieltjes integral representations for the bulk transport coefficients of discretized uniaxial polycrystalline materials in a setting suitable for direct numerical calculation. These computations involve the spectral measures of real, symmetric random matrices of the form $X_j\Gamma X_j$ and $X_j\Upsilon X_j$, $j = 1, 2$, where Γ and Υ are projections onto the range of the gradient and curl operators and are constructed from finite difference matrices. Meanwhile, X_1 is a random, real, symmetric projection matrix which encodes crystallite arrangement and orientation.

We show that the discrete mathematical framework describing effective transport for uniaxial polycrystalline materials closely parallels the continuum theory and showed the existence of transport fields \mathbf{E} and \mathbf{J} in discrete media follows from the fundamental theorem of linear algebra and the known orthogonality properties of the domains, ranges, and kernels of finite difference representations of the curl, gradient, and divergence operators. Resolvent representations of the transport fields enable explicit computation of \mathbf{J} in arbitrary polycrystalline geometries through eigenvalue decomposition of the matrices $X_1\Gamma X_1$ and $X_2\Gamma X_2$.

We developed an efficient projection method that demonstrates the spectral measures can be computed using matrices by a factor of d in each dimension, leading to considerable computational savings. We validated our framework through numerical calculations of spectral measures and the effective conductivity

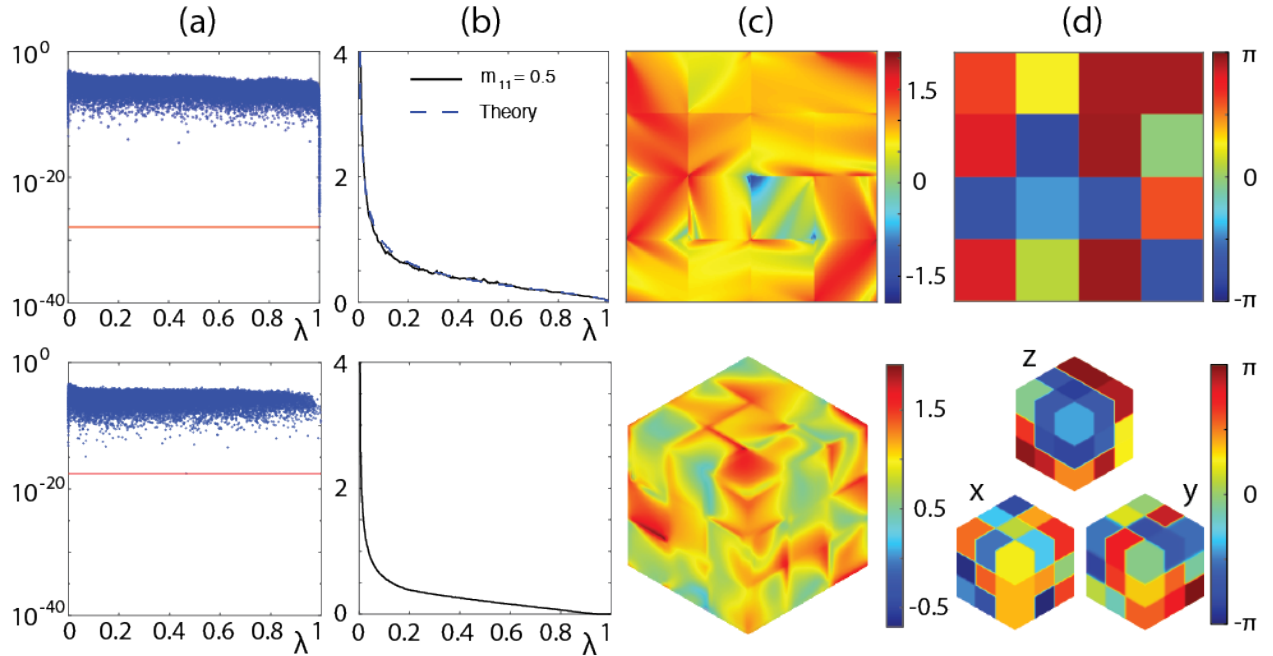


FIGURE 1. Spectral measures and current density fields for 2D (top row) and 3D (bottom row) uniaxial polycrystalline media. (a) Spectral measure weights m_i versus associated eigenvalue λ_i of the matrix M with corresponding current density field $|\mathbf{J}|$ in log10 scale shown in (c). The red horizontal lines in (a) correspond to the smallest weight m_i across the entire spectrum. The orientation of each crystallite (d) is taken to be uniformly distributed on the interval $[-\pi, \pi]$ from the x -axis (2D) and from the x , y , and z -axes (3D). The crystallite orientations in 3D are achieved through composed rotations along the x , y , and z axes in a random succession. (b) Corresponding spectral functions $\mu(\lambda)$ (histogram representations) of the spectral measure μ in (a), averaged over 2000 distinct geometric configurations. Each configuration is distinguished solely by the isotropic orientation angles $\theta_j \sim U[-\pi, \pi]$. In 2D, the geometric isotropy of the orientation angles allows the spectral function to align with the self-duality theoretical result $\mu_{kk}(\lambda) = (1/\pi)\sqrt{(1-\lambda)/\lambda}$. The electrical conductivity is taken to be $\sigma_1 = 51.074 + i45.160$ in the x direction and $\sigma_2 = 3.070 + i0.0019$ in the y and z directions. E_0 is taken to be oriented along the y -axis.

for both 2D and 3D uniaxial polycrystalline media with checkerboard microgeometry. Our results for the spectral function in the 2D case for isotropic crystallite orientations align closely with known self-duality results.

Acknowledgements. We gratefully acknowledge support from the Division of Mathematical Sciences at the US National Science Foundation (NSF) through Grants DMS-0940249, DMS-1413454, DMS-1715680, DMS-2111117, DMS-2136198, and DMS-2206171. We are also grateful for support from the Applied and Computational Analysis Program and the Arctic and Global Prediction Program at the US Office of Naval Research through grants N00014-13-1-0291, N00014-18-1-2552, N00014-18-1-2041 and N00014-21-1-2909.

REFERENCES

- [1] S. Barabash and D. Stroud. Spectral representation for the effective macroscopic response of a polycrystal: application to third-order non-linear susceptibility. *J. Phys., Condens. Matter*, 11:10323–10334, 1999.
- [2] D. J. Bergman. The dielectric constant of a composite material – A problem in classical physics. *Phys. Rep. C*, 43(9):377–407, 1978.
- [3] D. J. Bergman. Exactly solvable microscopic geometries and rigorous bounds for the complex dielectric constant of a two-component composite material. *Phys. Rev. Lett.*, 44:1285–1287, 1980.

- [4] D. J. Bergman. Rigorous bounds for the complex dielectric constant of a two-component composite. *Ann. Phys.*, 138:78–114, 1982.
- [5] C. Bonifasi-Lista and E. Cherkaev. Electrical impedance spectroscopy as a potential tool for recovering bone porosity. *Phys. Med. Biol.*, 54(10):3063–3082, 2009.
- [6] E. Cherkaev. Inverse homogenization for evaluation of effective properties of a mixture. *Inverse Problems*, 17(4):1203–1218, 2001.
- [7] E. Cherkaev and C. Bonifasi-Lista. Characterization of structure and properties of bone by spectral measure method. *J. Biomech.*, 44(2):345–351, 2011.
- [8] E. Cherkaev and K. M. Golden. Inverse bounds for microstructural parameters of composite media derived from complex permittivity measurements. *Waves in random media*, 8(4):437–450, 1998.
- [9] A. R. Day and M. F. Thorpe. The spectral function of composites: the inverse problem. *J. Phys., Condens. Matter*, 11:2551–2568, 1999.
- [10] J. W. Demmel. *Applied Numerical Linear Algebra*. SIAM, 1997.
- [11] K. M. Golden. Critical behavior of transport in lattice and continuum percolation models. *Phys. Rev. Lett.*, 78(20):3935–3938, 1997.
- [12] K. M. Golden. The interaction of microwaves with sea ice. In G. Papanicolaou, editor, *Wave Propagation in Complex Media, IMA Volumes in Mathematics and its Applications, Vol. 96*, pages 75–94. Springer – Verlag, 1997.
- [13] K. M. Golden, N. B. Murphy, and E. Cherkaev. Spectral analysis and connectivity of porous microstructures in bone. *J. Biomech.*, 44(2):337–344, 2011.
- [14] K. M. Golden and G. Papanicolaou. Bounds for effective parameters of heterogeneous media by analytic continuation. *Commun. Math. Phys.*, 90:473–491, 1983.
- [15] A. Gully, J. Lin, E. Cherkaev, and K. M. Golden. Bounds on the complex permittivity of polycrystalline materials by analytic continuation. *Proceedings of the Royal Society of London. Series A, Mathematical and physical sciences*, 471(20140702), 2015.
- [16] R. A. Horn and C. R. Johnson. *Matrix Analysis*. Cambridge University Press, 1990.
- [17] Tsung-Ming Huang, Wen-Wei Lin, and Weichung Wang. Matrix representations of discrete differential operators and operations in electromagnetism. *Ann. Math. Sci. Appl.*, 4(1):55–79, 2019.
- [18] J. D. Jackson. *Classical Electrodynamics*. John Wiley and Sons, Inc., New York, 1999.
- [19] R. C. McPhedran, D. R. McKenzie, and G. W. Milton. Extraction of structural information from measured transport properties of composites. *Applied Physics A: Materials Science & Processing*, 29(1):19–27, 1982.
- [20] R. C. McPhedran and G. W. Milton. Inverse transport problems for composite media. *MRS Proceedings*, 195, 1 1990.
- [21] G. W. Milton. Bounds on the complex dielectric constant of a composite material. *Appl. Phys. Lett.*, 37:300–302, 1980.
- [22] G. W. Milton. *Theory of Composites*. Cambridge University Press, Cambridge, 2002.
- [23] N. B. Murphy, E. Cherkaev, C. Hohenegger, and K. M. Golden. Spectral measure computations for composite materials. *Commun. Math. Sci.*, 13(4):825–862, 2015.
- [24] N. B. Murphy, E. Cherkaev, J. Zhu, J. Xin, and K. M. Golden. Spectral analysis and computation for homogenization of advection diffusion processes in steady flows. *Journal of Mathematical Physics*, 61(1):013102, 2020.
- [25] N. B. Murphy and K. M. Golden. The Ising model and critical behavior of transport in binary composite media. *J. Math. Phys.*, 53:063506 (25pp.), 2012.
- [26] N. Benjamin Murphy, Daniel Hallman, Elena Cherkaev, and Kenneth M. Golden. Spectral theory of effective transport for continuous uniaxial polycrystalline materials, 2024.
- [27] G. Papanicolaou and S. Varadhan. Boundary value problems with rapidly oscillating coefficients. In *Colloquia Mathematica Societatis János Bolyai 27, Random Fields (Esztergom, Hungary 1979)*, pages 835–873. North-Holland, 1982.
- [28] L. N. Trefethen and D. Bau. *Numerical Linear Algebra*. Society for Industrial and Applied Mathematics, 1997.
- [29] D. Zhang and E. Cherkaev. Reconstruction of spectral function from effective permittivity of a composite material using rational function approximations. *J. Comput. Phys.*, 228(15):5390–5409, 2009.